Nov 10th, 12:00 AM - 12:00 AM

Design of New Cold Rolled Purlins by Experimental Testing and Direct Strength Method

V. B. Nguyen

B. Cartwright

M. A. English

Wei-Wen Yu International Specialty Conference on Cold-Formed Steel Structures
Baltimore, Maryland, U.S.A, November 9 & 10, 2016

Design of new cold rolled purlins by experimental testing and Direct Strength Method

V.B. Nguyen[1], B. Cartwright[2] and M.A. English[3]

Abstract

New cold roll formed channel and zed sections for purlins, namely UltraBEAM^{TM}2 and UltraZED^{TM}2, have been developed by Hadley Industries plc using a combined approach of experimental testing, finite element modelling and optimisation techniques. The new sections have improved strength to weight ratio by increasing the section's strength by using stiffeners in the section webs. The European standards, Eurocode 3, use a traditional Effective Width Method to determine the strength of a cold formed steel member. However, the design of the new sections UltraBEAM^{TM}2 and UltraZED^{TM}2 using this method is very complicated in calculating the effective section properties as these sections contain complex folded-in stiffeners. In addition, the incorporation of competing buckling modes such as distortional buckling can be difficult to analyse. To overcome difficulties of using Eurocode 3 or such a standard with the Effective Width Method for the design of these sections, the Direct Strength Method (DSM) is adopted for determining the section strengths. Four-point beam bending tests were carried out to determine the buckling and ultimate bending capacity of the UltraBEAM^{TM}2 and UltraZED^{TM}2 sections. Results of experimental testing and Finite Element Analysis were initially used as validation for the design using the DSM. The DSM results in terms of in bending moment capacities were then compared with the experimental test results for a broader data in which the UltraBEAM^{TM}2 and UltraZED^{TM}2 sections had a range of different width-to-thickness ratios. It showed an excellent agreement between test and DSM design values. It is concluded that the DSM is a powerful tool for the design and optimisation of the new cold roll formed channel and zed purlins.

[1]Lecturer, Department of Engineering, University of Derby, Markeaton Street, Derby, DE22 3AW, UK.
[2]Product Development Manager, Hadley Industries plc, Smethwick, West Midlands, UK.
[3]Design and Development Manager, Hadley Industries plc, Smethwick, West Midlands, UK.

Introduction

Cold-formed purlin sections are usually manufactured into conventional channel and zed profiles. These sections consist of plate elements of the web and flanges which usually have a large width-to-thickness ratio. Therefore, they are prone to local or distortional buckling and this buckling governs the failure modes for cold-formed steel members. There have been extensive investigations on buckling and ultimate strengths of these conventional sections and practical design specifications are also available in codes of practice in different countries such as European Standard (EC3, 2006), North American Specification (NAS, 2007) and Australian/New Zealand Standard (AS/NZS, 2005).

To improve the strength of cold-formed sections that are prone to local / distortional buckling, stiffeners have been placed at the web of the sections. These stiffeners subdivide the plate elements into smaller sub-elements and hence can considerably increase the local buckling of cold-formed sections subjected to compressive stresses due to the smaller width-to-thickness ratio of the sub-elements. In recent years, there has been a significant number of studies on the strength and design of cold-formed sections with web stiffeners (Desmond et al. 1978, Papazian et al. 1994, Schafer and Pekoz 1998, Young and Chen 2008, Zhang and Young 2012). However, the majority of these studies are for columns under compression or hat sections under bending and there have been limited investigations on channel and zed sections with web stiffeners subjected to bending.

A zed section with longitudinal stiffeners in the web, introduced during cold rolled forming, was designed and developed at the University of Strathclyde by Rhodes and Zaras (1988) in conjunction with Hadley Industries plc, with the aim of improving the performance of a zed type section. The development suggested that when the stiffeners were placed about one fifth of the web width from each flange, the problem of local buckling in the web was eliminated. The channel section with longitudinal stiffeners in the web was developed at Hadley Industries plc later in an attempt to incorporate the innovative web stiffener configuration used in the new zed, into a channel shape (Castellucci et al. 1997). Recent investigations using Finite Element analysis (FEA) and optimisation techniques have proved that when the two symmetrical stiffeners on the web were placed closely to each flange, maximum buckling and ultimate strengths for the section were achieved (Nguyen et al. 2015). Since the sections evolved had the basic zed shape, Z, and channel shape, C, with additional enhancements which proved improved performance, they were decided that these sections should be named the 'UltraZED^{TM}2' and 'UltraBEAM^{TM}2' as illustrated in Figure 1, respectively from now on in this paper.

These new sections have a considerably improved strength to weight ratio considerably by using the web stiffener types as shown in Figure 1. Additional small stiffeners in zed sections that have large width-to-thickness ratios were added to introduce a greater degree of work hardening, which raises the material yield strength in these regions, taking increased further advantage of eliminating the local buckling. All of the current design codes including the European standard Eurocode 3 (EC3) use a traditional Effective Width Method (EWM) to determine the strength of a cold formed steel member. However, the design of the new sections UltraBEAM^{TM}2 and UltraZED^{TM}2 using this method is very complicated in calculating the effective section properties as these sections contain complex folded-in stiffeners. In addition, the incorporation of competing buckling modes such as distortional buckling can be difficult.

An alternative to the EWM is the Direct Strength Method (DSM) which is currently adopted in the North American Standard (NAS, 2007) and Australian/New Zealand standard (AS/NZS, 2005). The DSM uses the elastic buckling loads for the gross section considering local, distortional and global buckling to determine the strength of a cold-formed steel member. The DSM does not need to calculate the effective section properties; instead the elastic buckling analysis is calculated with computer aided numerical analysis so it can be used for design of cold-formed steel members with complex stiffeners (Schafer 2006). On the other hand, the DSM in current specifications is a semi-empirical approach, which was calibrated to cover only the pre-qualified sections specified in NAS (2007), and the UltraBEAM^{TM}2 and UltraZED^{TM}2 shapes are not in this list. Therefore, the DSM was adopted in this paper for design of the UltraBEAM^{TM}2 and UltraZED^{TM}2 purlins and was evaluated against experimental tests.

In this paper, four-point beam bending tests have been carried out to determine the ultimate bending capacity of the UltraBEAM^{TM}2 and UltraZED^{TM}2 sections which have a range of different geometries. Together with beam bending tests, tensile tests of the beam material were also conducted to determine the material properties. FE simulations of the bending tests of the UltraBEAM^{TM}2 and UltraZED^{TM}2 sections were presented. The DSM in current specifications was evaluated for the strength of the UltraBEAM^{TM}2 and UltraZED^{TM}2 sections based on the experimental and FE results.

Experimental test programme

The beam specimens were cold roll formed along the rolling direction on steel coils with a nominal Young's modulus of 205 GPa. Typical cross sections of the

test specimens are shown in Figure 1. Measured test section geometries and dimensions are given in Table 1 for UltraBEAM^{TM}2 sections and Table 2 for UltraZED^{TM}2 sections. Dimensional measurements were carried out and recorded for all test specimens prior to testing. This allows the exact profile geometry to be evaluated within the DSM and FE simulations. Measurements taken include material thickness, web width (or depth), flange width, and lip length.

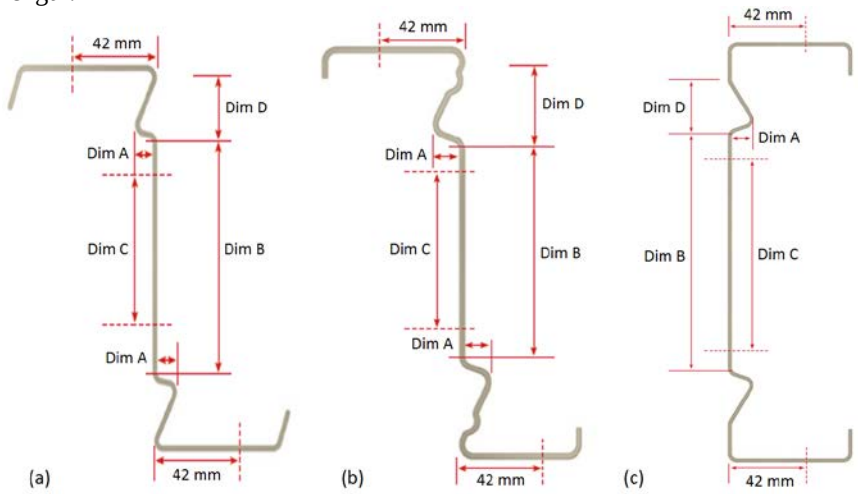

Figure 1 Cross sections and geometries of beam specimens (a) UltraZED^{TM}2 145-170 mm deep sections, (b) UltraZED^{TM}2 200-305 mm deep sections, and (c) UltraBEAM^{TM}2 145-305 mm deep sections. The depth of the section is also called the web width; Dim C is the hole centre

The beam specimens were labelled, an UltraBEAM^{TM}2 specimen label starts with C whilst an UltraZED^{TM}2 specimen starts with Z. For example, a specimen labelled as C-W145T1.2 is described as follows: C: Channel specimen; W: Web, 145: Nominal web height or beam depth (mm); T: Thickness, 1.2: Nominal plate thickness (mm). The forming process of each specimen is cold-rolled forming.

The material properties of the beam specimens were determined from tensile tests, adhering to Annex B of BS EN 10002-1:2001. Tensile test results in terms of yield stress, tensile strength and elongation are shown in Tables 1 and 2 for UltraBEAM^{TM}2 and UltraZED^{TM}2 steel materials, respectively. Experimental tests complying with standard BS EN 1993-1-3:2006 were carried out to evaluate the FE and DSM results. A typical test setup for the four-point bending test of is shown in Figure 2.

Table 1 Measured test section geometries and dimensions for UltraBEAM™2 sections

Channel sections				Flange		Dim A	Dim D	Dim B	Second Moment	Section modulus	Tensile Test Material Properties		
Section Reference	Thickness mm	Depth mm	Radius mm	Width mm	Lip mm	mm	mm	mm	Major axis mm^4x10^4	Major axis mm^3x10^3	Yield Stress N/mm^2	Tensile Strength N/mm^2	Elongation %
C-W145T1.2	1.23	145.04	2.30	63.07	16.05	9.00	20.00	75.00	121.54	16.76	485.50	530.00	14.00
C-W145T1.4	1.40	145.02	2.10	62.98	16.01	9.00	20.00	75.00	141.10	19.46	485.50	530.00	14.00
C-W145T2.0	1.99	145.01	1.50	63.05	16.01	9.00	20.00	75.00	198.64	27.40	485.10	515.00	15.00
C-W170T1.2	1.20	170.05	2.30	63.01	16.05	9.00	20.00	100.00	176.09	20.72	604.00	684.00	12.50
C-W170T1.5	1.50	169.80	2.00	62.99	15.94	9.00	20.00	100.00	218.66	25.72	557.00	575.00	14.00
C-W170T2.0	2.01	170.00	1.50	63.04	15.98	9.00	20.00	100.00	288.34	33.92	535.00	640.00	14.00
C-W255T1.4	1.40	254.90	3.00	75.00	19.03	12.50	30.00	155.00	742.64	58.25	431.70	466.50	12.00
C-W255T2.3	2.32	255.02	2.10	75.06	19.02	12.50	30.00	155.00	820.21	64.33	450.20	545.00	26.00
C-W255T3.0	2.98	255.01	1.40	74.97	19.07	12.50	30.00	155.00	1009.89	79.21	487.00	552.00	27.00

Table 2 Measured test section geometries and dimensions for UltraZED™2 sections

Zed Sections				Top flange		Bottom flange		Dim A	Dim D	Dim B	Second moment	Section modulus	Tensile test material properties		
Section Reference	Thickness mm	Depth mm	Radius mm	Width mm	Lip mm	Width mm	Lip mm	mm	mm	mm	Major axis mm^4x10^4	Major axis mm^3x10^3	Yield Stress N/mm^2	Tensile Strength N/mm^2	Elongation %
Z-W145T1.2	1.25	145.07	2.70	67.00	15.02	61.03	13.89	10.00	25.00	90.00	126.95	17.18	433.50	519.00	22.00
Z-W145T1.5	1.55	145.01	2.60	67.04	15.03	61.00	13.92	10.00	25.00	90.00	157.43	21.29	462.90	566.00	21.00
Z-W145T2.0	2.00	145.00	2.30	66.95	15.05	60.96	13.94	10.00	25.00	90.00	207.14	28.02	483.00	591.00	17.00
Z-W200T1.2	1.22	199.70	5.40	70.03	14.92	60.08	13.05	15.00	42.50	100.00	257.32	25.06	599.00	609.00	12.00
Z-W200T1.8	1.77	200.03	5.10	70.01	15.05	59.97	13.07	15.00	42.50	100.00	382.70	37.26	543.00	568.00	13.25
Z-W200T2.5	2.42	200.06	4.75	69.40	15.04	60.02	12.92	15.00	42.50	100.00	522.47	50.86	460.20	512.00	12.00
Z-W255T1.3	1.28	255.00	5.35	69.70	14.97	59.91	13.00	13.00	42.50	155.00	500.84	38.38	475.80	587.00	20.50
Z-W255T1.8	1.82	255.02	5.10	70.06	14.91	59.96	13.04	13.00	42.50	155.00	689.19	52.58	490.00	580.00	20.00
Z-W255T2.5	2.47	254.80	4.75	70.02	15.02	60.01	12.95	13.00	42.50	155.00	938.99	71.93	513.00	590.00	21.00

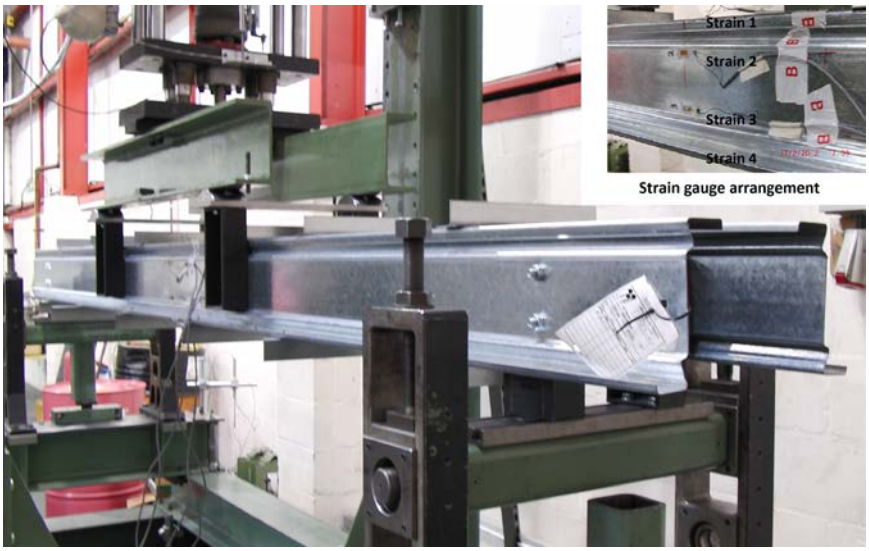

Figure 2 Four-point bending test setup, showing UltraZED^{TM}2 sections and strain gauge arrangement (in box)

A calibrated test rig was used for the tests. The rig consists of a 220-kN capacity load cell (LCHD-50K model, Omega Engineering Ltd.) and an electric machine screw jack. The beams were set up as simply supported beams. Rotating end station, as shown in Figure 2, was used to model the pin end condition of the beams at supports. Electrical strain gauges (SGD-10/120-LY11, Omega Engineering Ltd.) were used to measure the axial strains along the web and flanges of the cross section of the beam specimens; the critical buckling load was determined from strain gauge readings. Four strain gauges were mounted on the specimen mid-span, on the perimeter outside the specimen cross section, at the web positions close to the flanges and at the centres of flanges. LVDTs or displacement transducers were used for determining the vertical displacements from top and bottom of the beam specimens. Each test consists of two opposing sections (UltraBEAM^{TM}2 sections had their flanges faced inwards whilst UltraZED^{TM}2 sections had their top flanges faced inwards), allowing application of load through or close the shear centre of each section.

The load cell moved vertically down to apply a downward load symmetrically at two points at 0.33 x span centre. These loads were applied through the web of the section via a bolted connection using cleats, which in turn contacted the load cell beams via half round blocks, as shown in Figure 2, connected to cleats that

fixed to the beam webs. The load was spread to the beams via this cleat system. Half round blocks were used to ensure that the load applied to cleats was a point load. In this testing arrangement, pure in-plane bending of the beams could be obtained between the two loading points without the presence of shear and axial force. Dedicated cleat components allowed end connection rotation through supporting stations, and defined load point application at the centres of the beams.

Test spans adhere to the minimum requirements as stated in the standard. This distance was selected such that the ultimate load causing failure in the moment span is lower than that causing failure in the shear span. For accuracy during setting up, the beams were pierced during manufacture to allow fixing with M12 bolts (representative of those used in practice). The tested / manufactured spans are shown in Table 3. lateral restraints made of 45x45 mm angle were fixed by self-tapping screws to the top and bottom flanges at every 300-400 mm symmetrical to the mid-span and thereafter depending on beam depth and in turn the location of load points.

Table 3 Sample spans considered for testing and analysis

Section depth (mm)	145	170	200	225	255	285	305
Span (mm)	2295	2691	3087	3483	3879	4275	4275
Load centre (mm)	765	897	1029	1161	1293	1425	1425

Prior to each test the beam specimen was pre-loaded to remove any clearance in the connections, checking the alignment between specimens, connections and load cell. The applied load then returned to zero and the LVDTs and strain gauge readings were also set to zero. The specimen was loaded via the electric screw jack where displacement control was adopted to drive the load cell actuator at a constant rate of 2.5 mm/min. The specimen was loaded to failure and the test stopped at about 90% of the ultimate load. The data associated with load, displacement and strain gauge readings were recorded by the DASYLab data acquisition software (DASYLab software, Measurement Computing Corporation). Based on these data, load-deflection curves were plotted. To take into account the variation in sample and testing conditions, 4 duplicated tests were carried out. There were 116 tests in total for both UltraBEAM^{TM}2 and UltraZED^{TM}2 beams.

Direct Strength Method

The Direct Strength Method specified in the North American Specification (NAS, 2007) was used in this study to determine the bending moment capacities

of the UltraBEAM^{TM}2 and UltraZED^{TM}2 beams. This method considered elastic buckling loads identified from a numerical analysis. In particular, the finite strip software CUFSM software (2012) was used to identify the elastic buckling values for the beams. The elastic buckling analysis in CUFSM was performed for systematically increasing half-wavelengths to obtain the shapes and load factors for the buckling modes of the beam. Due to lateral restraints to the top and bottom flanges at every distance of 300-400 mm, no lateral-torsional buckling occurred to the beams in tests, so the beams were regarded as fully braced beams. Hence, the nominal flexural strength (M_{ne}) for lateral-torsional buckling was taken as the yield moment (M_y) for fully braced beams. The current DSM for beams that considered inelastic reserve capacities for local buckling and distortional buckling in the North American Specification were summarised as follows.

The ultimate flexural strength, M_n, is the minimum of nominal flexural strength due to global buckling (M_{ne}), nominal flexural strength for local buckling (M_{nl}) and nominal flexural strength for distortional buckling (M_{nd}), as shown as

$$M_n = \min(M_{ne}, M_{nl}, M_{nd}) \quad (1)$$

The nominal flexural strength for local buckling (M_{nl}) was calculated in accordance with the following:

$$\text{For } \lambda_l \leq 0.776,\ M_{nl} = M_y \quad (2)$$

$$\text{For } \lambda_l > 0.776,\ M_{nl} = [1-0.15(M_{crl}/M_y)^{0.4}](M_{crl}/M_y)^{0.4}M_y \quad (3)$$

Where $\lambda_l = (M_y/M_{crl})^{1/2}$; $M_y = S_f f_y$; S_f is the gross section modulus referenced to the extreme fiber at first yield; f_y is the yield stress which is the 0.2% proof stress ($\sigma_{0.2}$) obtained from tensile coupon tests in this study; M_{crl} is the critical elastic local buckling moment ($M_{crl} = S_f\sigma_{crl}$, in which σ_{crl} is the critical elastic local buckling stress).

The nominal flexural strength for distortional buckling (M_{nd}) was calculated in accordance with the following:

$$\text{For } \lambda_d \leq 0.673,\ M_{nd} = M_y \quad (4)$$

$$\text{For } \lambda_d > 0.673,\ M_{nd} = [1-0.22(M_{crd}/M_y)^{0.5}](M_{crd}/M_y)^{0.5}M_y \quad (5)$$

Where $\lambda_d = (M_y/M_{crd})^{1/2}$; M_{crd} is the critical elastic distortional buckling moment ($M_{crl} = S_f\sigma_{crd}$, in which σ_{crd} is the critical elastic distortional buckling stress).

The critical elastic local buckling stress σ_{crl} and critical elastic distortional buckling stress σ_{crd} were obtained from the finite strip software CUFSM. The measured cross-section dimensions and material properties presented in Tables 1 and 2 were used to determine the theoretical buckling load.

Finite Element Analysis

Finite Element simulations were conducted using Marc (MSC Software, version 2014) to simulate the four-point bending test of the beams. In this example, the UltraBEAM^{TM}2 specimens **C-W170T1.6** had a total length of 2920 mm, a span of 2691 mm, a load centre of 897 mm, thickness of 1.60 mm, flange width of 63 mm, web width of 170 mm and corner radius of 2.0 mm. Other beam specimens had dimensions and material properties as presented in Table 1. Figure 3 illustrates the FE model setup. By taking advantage of symmetry, only a half of the test system was modelled. The beams were presented by shell elements on its central plane with a thickness of 1.60 mm. In these simulations, the material properties of the sheet steel were obtained from physical tensile tests. The braces were modelled as rigid links connections. Load was applied on the two central cleats at their centroids using the displacement-controlled method while the two end supports were fully fixed in vertical direction at their centroids. Each loading point was at a reference node that connects to a set of tied nodes (at the beam web where the cleat connected to the beam). The link between the reference node and the tied nodes was based on a rigid link connection, only unrestrained in loading direction. Details of FE models were given in Nguyen et al. (2015).

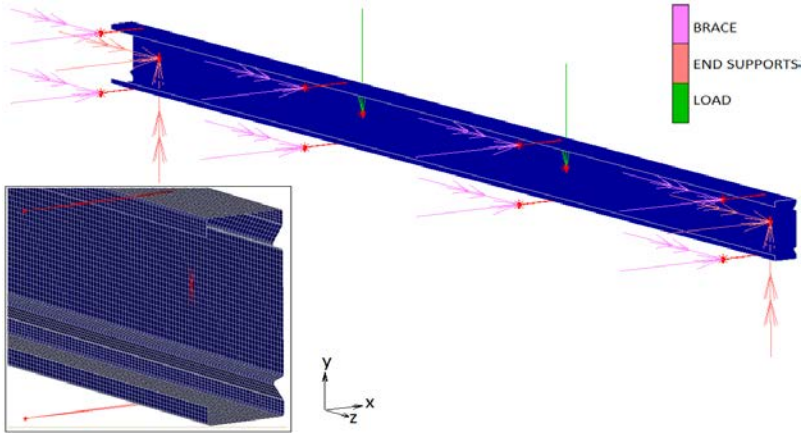

Figure 3 FEA four-point bending test setup including boundary conditions and a closer view of the mesh

Test results and discussion

Results of experimental tests, DSM and Finite Element simulations of beam specimens **C-W170T1.6** in the UltraBEAM^{TM}2 test group are presented first. Results of all UltraBEAM^{TM}2 and UltraZED^{TM}2 beams are presented in Table 4.

The results for the elastic buckling analysis using the software CUFSM are provided for the beam specimens **C-W170T1.6** in Figure 4. The first two minima indicate $M_{crl}/M_y = 1.25$ and $M_{crd}/M_y = 0.75$ which clearly shows that the distortional buckling is dominated the behaviour and failure mode of the beams.

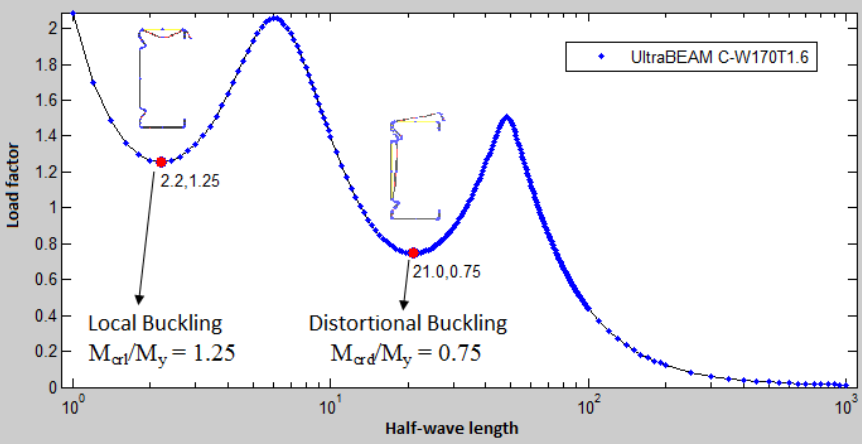

Figure 4 Buckling curves and modes of the UltraBEAM^{TM}2 specimens **C-W170T1.6** obtained from the software CUFSM

Figure 5 shows the comparison between the experimental, DSM and FE results for the UltraBEAM^{TM}2 specimens. The experimental and FE load-displacement curves were also plotted for comparison. The DSM and FE results were similar in both buckling and ultimate loads, with a maximum difference of less than 2% in buckling load and 4% in ultimate load. The DSM ultimate load was in excellent agreement with experimental value for ultimate load, with a maximum difference of 3%. However, for this particular example the test did not clearly show elastic buckling prior to failure. It was noted that the buckling loads obtained from the DSM (or more accurate, the finite strip analysis) and FE analysis were even greater than the ultimate loads. The main reason for this could be the fact that the tested beams deformed in plastic region while the DSM and FE local buckling loads were evaluated by means of linear elastic analysis.

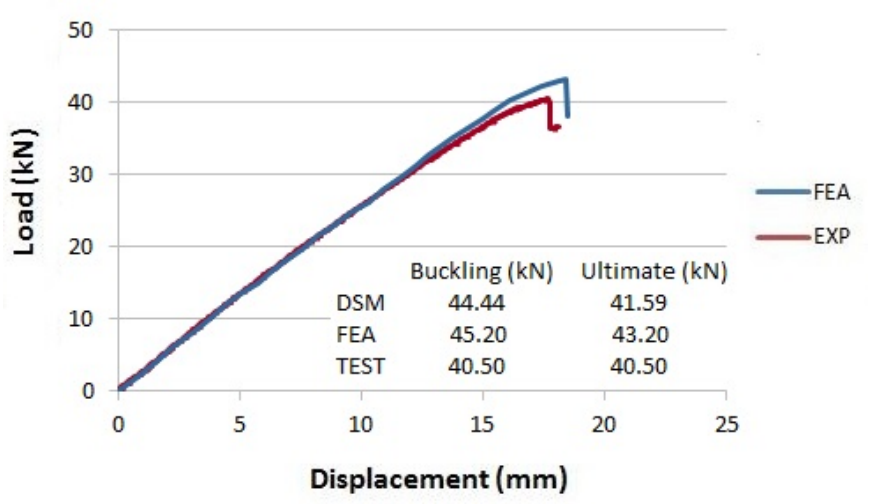

Figure 5 Results of experimental test, DSM and FEA, including load-displacement curves for the UltraBEAM^{TM}2 specimens **C-W170T1.6**

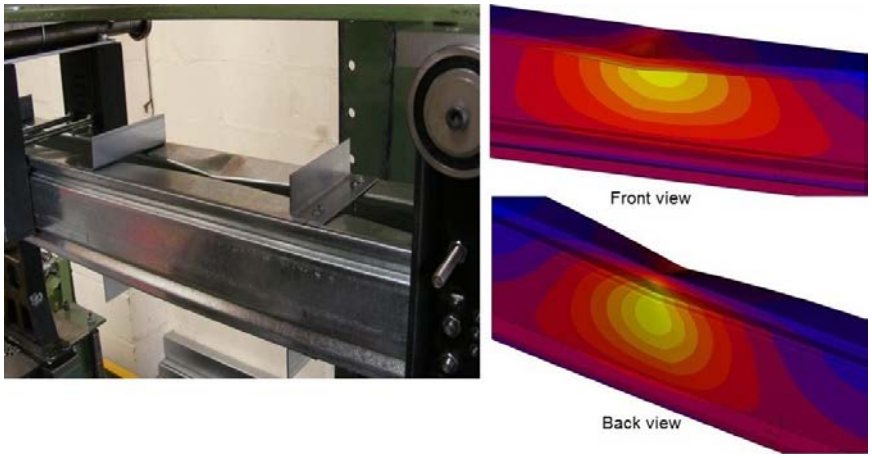

Figure 6 Failed mode shapes of the UltraBEAM^{TM}2 in testing and FE simulation. Displacement contour is presented in FE results in which lighter colours indicate greater displacement magnitudes

Figure 6 shows the failed mode shapes of the UltraBEAM^{TM}2 in comparison with the experimental shapes. It can be seen that the buckling and failed modes

predicted by DSM and FE models are very similar to the experimental modes. This further confirms the validation of the DSM and FE simulations. Figures 5 and 6 also show that the beam specimens had similar buckling failure modes in DSM and FEA although in DSM the flanges came out and the web came in, which are in opposite directions to the experimental and FEA modes.

Table 4 Comparison of moment capacities obtained from DSM and test results. 'L', 'D', 'F' stand for 'Local buckling', 'Distortional buckling' and 'Full section', respectively

Specimens	Test		DSM		Comparison
	M_{EXP} (kNm)	Failed mode	M_{DSM} (kNm)	Failed mode	M_{EXP}/M_{DSM}
(1)	(2)	(3)	(4)	(5)	(6)
UltraBEAM™2					
C-W145T1.2	5.97	D	6.21	D	0.96
C-W145T1.4	6.54	D	6.03	D	1.08
C-W145T2.0	9.57	D	9.99	D	0.96
C-W170T1.2	6.04	D	6.58	D	0.92
C-W170T1.5	8.43	D	8.64	D	0.98
C-W170T1.6	9.08	D	9.33	D	0.97
C-W170T2.0	12.75	D	12.73	D	1.00
C-W255T1.5	11.55	D	11.68	D	0.99
C-W255T2.3	23.82	D	24.67	D	0.97
C-W255T3.0	40.09	D	38.10	D	1.05
UltraZED™2					
Z-W145T1.2	7.29	F	7.81	F	0.93
Z-W145T1.5	9.50	F	9.69	F	0.98
Z-W145T2.0	12.35	F	12.76	F	0.97
Z-W200T1.2	10.75	F	11.49	F	0.94
Z-W200T1.8	17.07	F	17.04	F	1.00
Z-W200T2.5	22.20	F	23.32	F	0.95
Z-W255T1.3	16.50	D	16.29	D	1.01
Z-W255T1.8	23.18	F	23.96	F	0.97
Z-W255T2.5	31.98	F	32.86	F	0.97

Table 4 shows the results of moment capacities of all UltraBEAM™2 and UltraZED™2 beams obtained from experimental test (M_{EXP}) and Direct Strength Method (M_{DSM}). The comparison between these values is shown in column (6)

of Table 4. Comparison of the DSM results with experimental test results shows a minimum variation of 0% up to a maximum of 8%. The average variation in bending moment achieved through the DSM and physical testing is 4% for all data with the DSM giving conservative results in 3/19 cases. In particular, the DSM and experimental values were similar, with maximum differences of 8% and 7% for UltraBEAM^{TM}2 and UltraZED^{TM}2 specimens, respectively. In addition, the modes of failure observed during experimental tests were similar to those obtained from the DSM calculations, as shown in columns (3) and (5). In experimental tests of UltraBEAM^{TM}2 specimens, it was observed that as the load increased, wavelike deflections appeared along the length of the flanges and of the beam specimens, and the flange edges bent down; these beam specimens clearly exhibited 'distortional buckling'. However, for many UltraBEAM^{TM}2 beams, this phenomenon happened fast and followed by failure of the beams. These show a very good agreement between test and DSM design values. Trends have been identified between bending moment capacity and depth-to-thickness ratio for a range of UltraBEAM^{TM}2 and UltraZED^{TM}2 beams from both experimental and DSM results. A decrease in depth-to-thickness ratio shows an increase to bending moment capacity for the given depth-to-thickness range. This has been shown for the UltraBEAM^{TM}2 and UltraZED^{TM}2 sections in columns (2) and (4), respectively.

Table 5 Failure modes identified from DSM for 305 mm deep UltraZED^{TM}2 range

Section Depth	Thickness	Bending Moment	Depth-to-thickness Ratio	Failure Mode	Reduction in capacity
(mm)	(mm)	(kNm)			(%)
305	1.50	22.34	203.33	Distortional Buckling	-13%
305	1.60	24.32	190.63	Distortional Buckling	-11%
305	1.80	28.35	169.44	Distortional Buckling	-8%
305	2.00	32.51	152.50	Distortional Buckling	-4%
305	2.30	38.80	132.61	Full section capacity	0%
305	2.50	42.01	122.00	Full section capacity	0%
305	3.00	49.92	101.67	Full section capacity	0%

The depth-to-thickness ratio shows a relationship between the exhibited failure modes within a section range. Sections with the lowest depth-to-thickness ratio

show a fully effective section capacity, while the higher depth-to-thickness ratios show a reduced section capacity caused by local and distortional buckling effects. Where buckling effects are dominant the effective section modulus will be used to calculate the moment capacity. Where the full section capacity is dominant the gross section modulus will be used to calculate the section capacity. This has been shown for the 305mm deep zed profile range in Table 5. Observations from Table 5 show that sections with a higher depth-to-thickness ratio exhibited greater effects from buckling than sections with a lower depth-to-thickness ratio. The magnitude of capacity reduction generated from buckling effects is between 0% and 13% for UltraZED^{TM}2 sections, and between 5% and 37% for UltraBEAM^{TM}2 sections.

Conclusions

The experimental test and design by the Direct Strength Method for the new channel and zed purlins with web stiffeners namely UltraBEAM^{TM}2 and UltraZED^{TM}2 were presented. Simply supported UltraBEAM^{TM}2 and UltraZED^{TM}2 beams were tested under four-point bending about the major axis of the sections. In addition to experimental tests, a non-linear finite element model was developed and verified against the test results. The DSM was first evaluated by comparing its predicted bending moment capacities with those of test and finite element analysis for a four-point bending test of UltraBEAM^{TM}2 sections. The comparison shows excellent agreements between the DSM results and test and finite element results, including failed modes. Based on this validation, the DSM was used to predict strength of a wide range of UltraBEAM^{TM}2 and UltraZED^{TM}2 sections in terms of bending moment capacities and results were compared with test results. A total of 19 different purlin sections including 10 specimens of UltraBEAM^{TM}2 and 9 UltraZED^{TM}2 sections were investigated. Each section with the same depth had three different thicknesses that ranged from 1.20 mm to 3.05 mm in order to cover a wide popular range of section slenderness used in building construction. The overall beam depth-to-thickness ratios were studied. Four duplicated tests were carried out for each section so there were 116 tests in total for both UltraBEAM^{TM}2 and UltraZED^{TM}2 purlins.

Comparison of the DSM results with physical test results shows a minimum variation of 0% up to a maximum of 8%. The average variation in bending moment achieved through the DSM and experimental testing is 4% with the DSM giving conservative results in 3/19 cases. This shows that the nominal moment capacities predicted using the DSM are very comparable with test results for the UltraBEAM^{TM}2 and UltraZED^{TM}2 purlins subjected to bending. Therefore, it is recommended that the current Direct Strength Method in the

North American Standard (NAS, 2007) can be used for the strength design of cold roll formed UltraBEAM™2 and UltraZED™2 purlins subjected to bending.

References

AISI Standard. North American Specification for the Design of Cold-Formed Steel Structural Members. 2007 Edition.

AS/NZS 4600:2005. Australian/New Zealand standard cold-formed steel structures.

BS EN 10002-1:2001. Metallic materials - Tensile testing - Part 1: Method of test at ambient temperature.

BS EN 1993-1-3:2006. Eurocode 3 – Design of steel structures. Part 1-3: General rules – Supplementary rules for cold-formed members and sheeting.

Castellucci MA, Pillinger I, Hartley P, Deeley GT. The optimisation of cold rolled formed products. Thin-Walled Structures 1998;1-4:159-174.

CUFSM, version 4.05; 2012. URL: http://www.ce.jhu.edu/bschafer/cufsm/ (latest updated on 24th May 2012).

Desmond TP, Pekoz T., Winter G. Local and overall buckling of cold formed compression members. Department of Structural Engineering Report, Cornell University 1978.

Nguyen VB, English MA, Castellucci MA. FE simulation techniques for new process and product developments in metal forming industry. Proceedings of the 13th International Cold Forming Congress 2015;178-185.

Papazian RP, Schuster RM, Sommerstein M. Multiple stiffened deck profiles. Proceedings of the 12th International Specialty Conference on Cold-Formed Steel Structures 1994;217-228.

Rhodes J, Zaras J. Development and design analysis of a new purlin system. Proceedings of the 9th International Specialty Conference on Cold-Formed Steel Structures 1988;215-228.

Schafer BW, Adany S. Buckling analysis of cold-formed steel members using CUFSM: conventional and constrained finite strip methods. Proceedings of the 18th International Specialty Conference on Cold-Formed Steel Structures 2006;39-54.

Schafer BW, Pekoz T. The behaviour and design of longitudinally stiffened thin-walled compression elements. Thin-Walled Structures 1998;27:65-87.

Schafer BW. Designing cold-formed steel using the direct strength method. Proceedings of the 18th International Specialty Conference on Cold-Formed Steel Structures 2006.

Young B, Chen J. Design of cold-formed steel built-up closed sections with intermediate stiffners. Journal of Structural Engineering 2008; 134:727-737.

Zhang JH, Young B. Compression tests of cold-formed steel I-shaped open sections with edge and web stiffeners. Thin-Walled Structures 2012;52:1-11.